

DCVSMNet: Double Cost Volume Stereo Matching Network

Mahmoud Tahmasebi

*Centre for Mathematical Modelling and Intelligent Systems for Health and Environment (MISHE),
Atlantic Technological University
Sligo, Ireland*

MAHMOUD.TAHMASEBI@RESEARCH.ATU.IE

Saif Huq

*Department of Electrical, Computer Engineering, and Computer Science
York College of Pennsylvania
Pennsylvania, USA*

SHUQ@YCP.EDU

Kevin Meehan

*Department of Computer Science
Atlantic Technological University
Donegal, Ireland*

KEVIN.MEEHAN@ATU.IE

Marion McAfee

*Centre for Mathematical Modelling and Intelligent Systems for Health and Environment (MISHE),
Atlantic Technological University
Sligo, Ireland*

MARION.MCAFEE@ATU.IE

Abstract

We introduce Double Cost Volume Stereo Matching Network(DCVSMNet¹) which is a novel architecture characterised by two small upper (group-wise) and lower (norm correlation) cost volumes. Each cost volume is processed separately, and a coupling module is proposed to fuse the geometry information extracted from the upper and lower cost volumes. DCVSMNet is a fast stereo matching network with a 67 ms inference time and strong generalization ability which can produce competitive results compared to state-of-the-art methods. The results on several benchmark datasets show that DCVSMNet achieves better accuracy than methods such as CGI-Stereo and BGNet at the cost of greater inference time.

1 Introduction

Stereo matching networks attempt to mimic human vision perception of depth. Depth information is fundamental for environment perception in robots, autonomous vehicle navigation, and augmented reality applications. Stereo matching is a vision-based algorithm which enables formation of a three-dimensional (3D) reconstruction of the environment from two rectified stereo images. The stereo matching pipeline takes two rectified images as inputs to a feature extractor module. The extracted convolutional neural network (CNN) features are used to form a cost volume along with the disparity values. This cost volume stores fused information of left and right features to encode local matching costs. This information is further processed by an aggregation block and regressed to estimate the disparity map.

While stereo matching models can be roughly classified based on their speed and accuracy, there is no clear distinction between models which can be considered 'fast' or 'accurate' because these terms are highly dependent on the target application and available technology. For instance, applications

1. The source code is available at <https://github.com/M2219/DCVSMNet>.

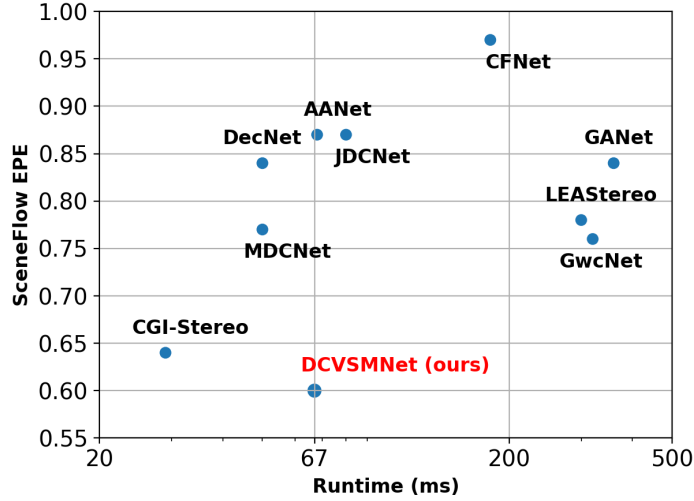


Figure 1: Comparison of DCVSMNet with state-of-the-art methods on SceneFlow dataset.

such as autonomous vehicles demand stereo models with high speed to mimic human-like perception of depth [1], on the other hand, many medical applications designed based on stereo endoscopy and stereo microscopy require higher accuracy depth prediction to improve surgical precision and patient safety with no need for a fast inference time [2]. To this end, research into deep learning stereo matching models involves continuously testing and adopting various strategies to trade off between the speed and accuracy for different target applications.

Considering the first block of the stereo matching pipeline which is feature extraction, designing smaller feature extractors composed of fewer convolutional layers can lead to a fast inference time at the cost of forming a poor cost volume and eventually less accurate prediction ability [3]. The produced cost volume is usually four dimensional which requires expensive 3D convolutions for cost aggregation. The computational effort and storage cost grows exponentially as the number of 3D convolutional layers increase. Therefore, the size of the cost volume directly affects both the speed and accuracy. The factor that controls the size of cost volume is the number of features used for the cost volume formation. Using the features from only a single scale of the feature extractor [1, 4, 5] leads to a smaller cost volume and faster inference time than a cost volume formed by concatenating features from several scales. The latter results in storing richer matching information and produces a more accurate disparity map but at the cost of higher computation effort [6, 7, 8, 9]. Modelling approaches which focus on high accuracy tend to construct several cost volumes which are further processed separately [10, 11] or are merged to form a big and well informed cost volume [6, 12, 13]. However, while such a large cost volume contains a great amount of useful matching information, it is also prone to storing a large amount of irrelevant information. Therefore, filtering big cost volumes to preserve richer matching information and suppress less important parameters is a direction taken by some researchers [14, 15, 16]. However, while filtering the cost volume to weaken irrelevant values increases the disparity estimation accuracy, it does not reduce the computation because the size of the cost volume is not changed after filtering. To alleviate this issue, one may consider designing an algorithm to remove insignificant information and reduce the size of cost volume. For example, MDCNet [17] and JDCNet [18] narrow the cost volume disparity range by comparing a pixel with its surroundings using a predefined threshold to remove irrelevant parameters. In another work,

SCV-Stereo [19] introduces a sparse cost volume that only stores the best K matching costs for each pixel by using k -nearest neighbors. The downside of such algorithms is that, while they reduce the size of the cost volume and increase the speed, some useful information will be lost together with unimportant parameters. One approach to overcome the deficiencies of using small feature extractors, cost volume filtering and cost volume dimension reduction, is to guide the aggregation block with contextual information stored in the different scales of the feature extractor [20, 21] or edge cues [22] and semantic information [23] extracted from the features. The guided aggregation block fuses the contextual information with the geometry information extracted from the cost volume which improves the estimation accuracy. Although such a fusion leads to better accuracy, the fusion module which is usually made of convolutional layers or Gated Recurrent Unit (GRU) convolutions [24] adds extra computation to the pipeline.

This research proposes a novel fast stereo matching network architecture with high level of accuracy and 67 ms inference time that we call DCVSMNet (see Fig.1). As shown in Fig.2, DCVSMNet is comprised of two upper and lower small cost volumes to reduce computation burden compared to a single large cost volume. The idea is to store rich matching information extracted from features in two cost volumes built using two different methods, group-wise correlation and correlation cost volumes. The cost volumes are aggregated separately and the obtained geometry information from the upper and lower cost volume are fused by a coupling module at different scales to help the network learn more accurate contextual information to achieve accurate disparity estimation. The summation of the upper and lower branch outputs is regressed to generate the final disparity map. DCVSMNet exhibits a competitive accuracy compared to other state-of-the-art methods with an inference time less than or equal to 80 ms when tested on high end GPUs. Our network can generalize very well to real-world datasets such as KITTI 2012 [25], KITTI 2015 [26], ETH3D [27] and Middlebury [28] when only trained on the SceneFlow [29] dataset, and outperforms fast networks such as CGIStereo [20], CoEx [16] and Fast-ACVNet [14].

Our main contributions are:

- We propose a double cost volume stereo matching pipeline which is capable of processing two small cost volumes using two light 3D networks to achieve a high level of accuracy by providing the network with richer matching cost information in comparison with a single large cost volume.
- We design a coupling module to fuse the geometry information extracted from two different cost volumes, enabling the network to learn more complex geometry and contextual information.
- We design a fast and accurate stereo matching network which outperform state-of-the-art methods (<80 ms) with a strong generalization ability.

2 Related work

DCVSMNet merges the left and right features to build two different cost volumes which can be categorized as the multi cost volumes approach. Using multi-scale information is widely used in computer vision tasks. For example, DeepLab [30] uses multi-scale features to improve semantic segmentation. SpyNet [31] and PWC-Net [32] employ mutli-level information extracted from features at different scales to compute optical flow. Using multiple cost volumes constructed from left and right features in the stereo matching domain has also shown a promising improvement in the disparity estimation. [3, 33, 34] propose a three-stage disparity refinement by constructing three cost volumes. The disparity of each stage (residual disparity) is used to warp the cost volume at the next

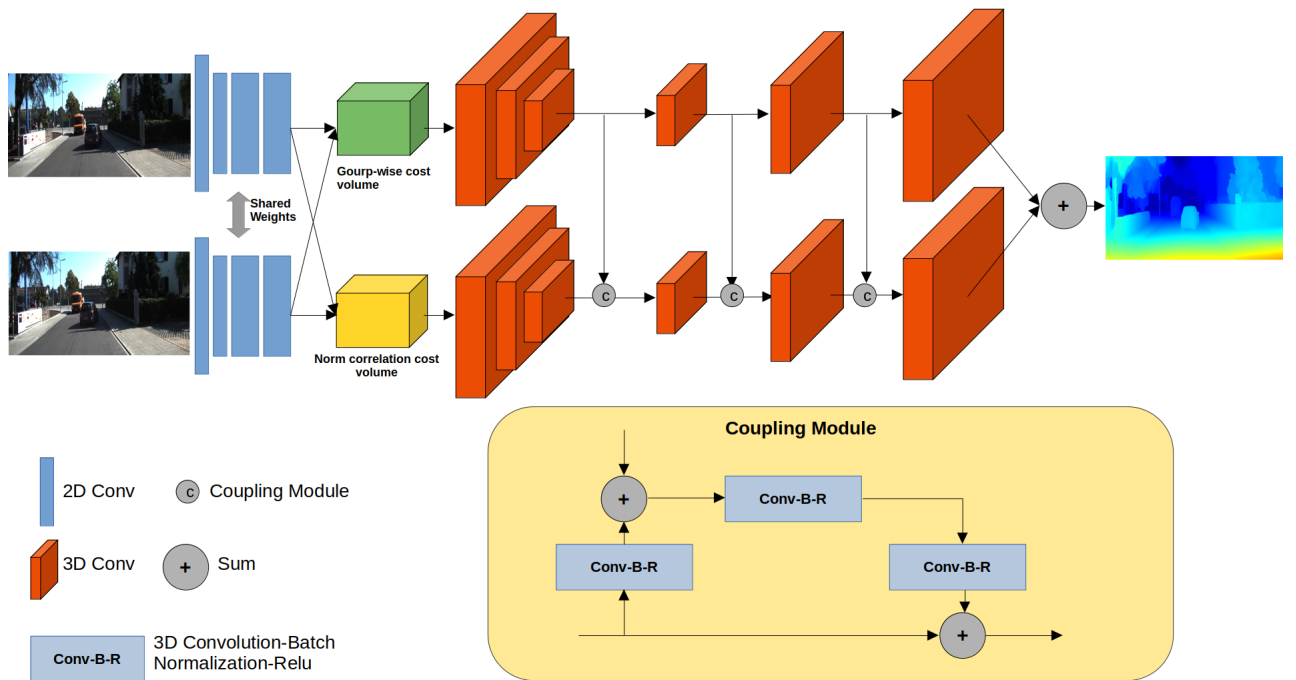


Figure 2: DCVSMNet uses both group-wise and norm correlation cost volumes to store rich matching cost information. Each volume is processed using a 3D hourglass network. The geometry information extracted from the upper and lower cost volume is fused by a coupling module and the final disparity map is generated by regressing the summation of the upper and lower branch outputs

stage to progressively update the disparity map. In comparison our method, DCVSMNet, uses the upper and lower cost volume to predict disparity in a single stage by removing the warping algorithm and taking advantage of a fusion module which results in outperforming these methods with better accuracy and speed. SSPCV-Net [35] builds a cost volume based on semantic segmentation information and three pyramidal cost volumes using features which are processed by a 3D-multi-scale aggregation network which is highly computational. MASNet [36] also uses semantic segmentation clues to refine the disparity estimation, however, the aggregation module includes three stacked 3D hourglass networks which adds to the computational burden of the network [37]. AANet [9] produces multi-scale cost volumes from features. The cost volumes are aggregated by six stacked Adaptive Aggregation Modules (AAModules). Each module consists of three Intra-Scale Aggregation (ISA) modules to alleviate the well-known edge-fattening issue at disparity discontinuities, and a Cross-Scale Aggregation (CSA) module which can extract information in textureless regions. However, while the computational burden imposed by the ISA and CSA modules in AANet is at the level of our coupling module, DCVSMNet gains much better accuracy with the same inference time (see Fig. 1). ADCPNet [38] constructs a full range and a compact cost volume to predict the disparity using a two-stage coarse-to-fine framework. ADCPNet sacrifices the accuracy over speed by aggressively limiting the disparity range for forming a compact cost volume, which results in a faster but less accurate network compared to DCVSMNet. The closest work to our approach is GWCNet [6]. GWCNet constructs a group-wise as well as a concatenation cost volume. Further, the two cost volumes are merged to build a single combined cost volume which is processed by three 3D stacked hourglass networks. Motivated by GWCNet, our approach is powered by two parallel low-resolution cost volumes built by the merged left and right features. The upper cost volume is a group-wise cost volume with a half of the size of volume used in GWCNet and the lower cost volume is a norm correlation cost volume which is aggressively compressed using a 3D convolution layer. Finally, instead of merging the two cost volumes, they are separately processed using two light aggregation networks which are connected by a coupling module for fusing the geometry information.

3 Method

As shown in Fig.2, DCVSMNet takes two stereo pair images as input and the contextual information is extracted using a ResNet-like network. The features are used to build two low-resolution cost volumes aggregated by two parallel 3D hourglass networks which are fused using a coupling module to extracted high-resolution geometry features. The summation of the upper and lower branch output is regressed to estimate the final disparity map. In this section, we first introduce the architecture of the coupling module (Sec.3.1). The feature extraction architecture and the construction of cost volumes is described in section 3.2. Then, the architecture of the aggregation network is discussed in section 3.3. Finally, we explain the disparity regression and the loss function used to train our architecture in sections 3.4 and 3.5.

3.1 Coupling Module

To extract accurate and high-resolution geometry information from two low-resolution cost volumes, we propose a coupling module to fuse the information of the upper and lower branches extracted from the decoder module of the aggregation networks.

The output features at each scale of the aggregation’s decoder module are used as the inputs of the coupling module. Considering $G_u \in \mathbb{R}^{B \times C_u \times D_u \times H_u \times W_u}$ and $G_l \in \mathbb{R}^{B \times C_l \times D_l \times H_l \times W_l}$ as two geometry features extracted from the upper and lower branch subscribed by u and l , where B is the batch size, D is the disparity range, C , H and W are the number of channels, feature height and width. The coupling module takes G_u and G_l as inputs and fuse the information based on Eq.1,

where, $f_1^{3 \times 3}$ and $f_2^{3 \times 3}$ are convolution operations with the filter size $1 \times 3 \times 3$ (see Fig.2). Eq.1 results in fused geometry features G_{fused} with the same dimension as G_l and G_u .

$$G_{fused} = f_1^{3 \times 3}(f_2^{3 \times 3}(G_l) + G_u) + G_l \quad (1)$$

3.2 Feature Extraction and Cost Volumes

DCVSMNet adopts the PSMNet [39] feature extraction backbone with the half dilation settings, ignoring its spatial pyramid pooling module. The output features are $\frac{1}{4}$ resolution of the input images. The last three scales of the feature extraction are concatenated to generate a 320-channel feature map. Following GWCNet [6], to form a group-wise cost volume, the feature map is split to N_g groups along the channel dimension. Considering the number of feature map channels as N_c , g th feature group as f_l^g and f_r^g , the group-wise cost volume can be formed as Eq.2.

$$C_{gwc}(d, x, y, g) = \frac{N_g}{N_c} \langle f_l^g(x, y), f_r^g(x - d, y) \rangle \quad (2)$$

$\langle \cdot, \cdot \rangle$ denotes the inner product, d is the disparity index and (x, y) represents the pixel coordinate. The dimension of the generated cost volume is $[D_{max}/4, H/4, W/4, N_g]$, where, D_{max} is the maximum disparity. In addition, to form the norm correlation cost volume, the concatenated features are passed through a convolution operation followed by a BatchNorm and leaky ReLU to aggressively compress the channels from 320 to 12. Then, the norm cost volume is constructed using Eq.3, which has the dimension of $[D_{max}/4, H/4, W/4, 1]$.

$$C_{corr}(:, d, x, y) = \frac{\langle f_l(:, x, y), f_r(:, x - d, y) \rangle}{\|f_l(:, x, y)\|_2 \cdot \|f_r(:, x, y)\|_2} \quad (3)$$

3.3 Cost Aggregation

To extract high-resolution geometry information, two UNet-like (3D hourglass [14]) networks are used for aggregating the matching costs stored in the cost volumes. Each aggregation block consist of an encoder and a decoder module. The encoder module is made of three down-sampling layers and each layer includes a 3D convolution layer with kernel size $3 \times 3 \times 3$ with stride 2 followed by another 3D convolution layer with kernel size $3 \times 3 \times 3$ and stride 1. The encoder module reduces computation and using layers with stride 2 leads to increasing receptive field, which is a measure of association of the output layer to the input region. The decoder module is made of three up-sampling layers including $4 \times 4 \times 4$ 3D transposed convolution with stride 2 followed by $3 \times 3 \times 3$ 3D convolution with stride 1. To fuse geometry information extracted from two cost volumes, the output of each up-sampling layer of the upper branch is used as the input for coupling module which is alternatively employed after each up-sampling layer of the lower branch. Finally, the summation of the outputs from the upper and lower branch is fed to a regression block to compute the expected disparity map.

3.4 Disparity Regression

The aggregated cost volume is regularized by selecting top-k values at every pixel. To reduce the computation, the model is designed to compute the disparity map d_0 at $\frac{1}{4}$ resolution of the input images with $k = 2$. Then, d_0 is upsampled using weighted average of the "superpixel" surrounding each pixel to obtain the full resolution disparity map denoted as d_1 [16].

3.5 Loss Function

DCVSMNet is trained end-to-end and supervised by the weighted loss function described in Eq.4, where, d_0 is the estimated disparity map at $\frac{1}{4}$ resolution, d_1 is the expected disparity map at full resolution and d_{gt} is the ground truth disparity.

$$L = \lambda_0 smooth_{L_1}(d_0 - d_{gt}) + \lambda_1 smooth_{L_1}(d_1 - d_{gt}) \quad (4)$$

4 Experiment

In this section four datasets are introduced for evaluating DCVSMNet performance and studying the generalization ability.

4.1 Datasets and Evaluation Metrics

SceneFlow [29] is a synthetic dataset including 35454 training image pairs and 4370 testing image pairs with the resolution of 960×540 . The performance evaluation on SceneFlow is measured by End-Point Error (EPE) described in Eq.5 in which (x, y) is the pixel coordinate, d is the estimated disparity, d_{gt} is the ground truth disparity and N is the effective pixel number in one disparity image. Another metric that is used for evaluation on SceneFlow is disparity outlier (D1), which is defined as the pixels with errors greater than $max(3px, 0.05d_{gt})$. Because SceneFlow is a large dataset, it is widely used for pre-training stereo matching networks before fine-tuning on real-world benchmarks.

$$EPE = \frac{\sum_{(x,y)} |d(x, y) - d_{gt}(x, y)|}{N} \quad (5)$$

KIITI includes two benchmarks KIITI 2012 [25] and KITTI 2015 [26]. KITTI 2012 contains 194 training stereo image pairs and 195 testing images pairs, and KITTI 2015 contains 200 training stereo image pairs and 200 testing image pairs. KITTI datasets are a collection of real-world driving scene and provide sparse ground-truth disparity measured by LiDAR. For KIITI 2015, D1-all (percentage of stereo disparity outliers in the reference frame), D1-fg (percentage of outliers averaged only over foreground regions), and D1-bg (percentage of outliers averaged only over background regions) metrics are used for evaluation. For KIITI 2012, Out-Noc (percentage of erroneous pixels in non-occluded areas), Out-All (percentage of erroneous pixels in total), EPE-noc (end-point error in non-occluded areas), EPE-all (end-point error in total) are used for evaluation.

ETH3D [27] contains 27 training and 20 testing grayscale image pairs with sparse ground-truth disparity. The disparity range of ETH3D is 0-64 and the percentage of pixels with errors larger than 1 pixel (bad 1.0) is used for performance evaluation on ETH3D dataset.

Middlebury 2014 [28] is a collection of 15 training and testing indoor image pairs at full, half, and quarter resolutions. the percentage of pixels with errors larger than 2 pixels (bad 2.0) is reported as the metric for evaluation on this dataset. bad- σ error can be defined as Eq.6.

$$bad - \sigma = \frac{\sum_{(x,y)} |d(x, y) - d_{gt}(x, y)| > \sigma}{N} * 100\% \quad (6)$$

4.2 Implementation Details

DCVSMNet is implemented using PyTorch trained and evaluated on a single NVIDIA RTX 3090 GPU. The ADAM [40] method with $\beta_1 = 0.9$ and $\beta_2 = 0.999$ is used for optimization. The loss

Table 1: Ablation study on SceneFlow test set, the Baseline is the DCVSMNet architecture without the coupling module.

Method	Coupling Module	EPE[px]	D1[%]	>1px[%]	>2px[%]	>3px[%]	Time[ms]
Baseline	✗	0.72	2.60	7.98	4.35	3.18	65
DCVSMNet	✓	0.60	2.11	6.62	3.60	2.62	67

function’s weights are selected as $\lambda_0 = 0.3$ and $\lambda_1 = 1.0$. First, DCVSMNet is trained on SceneFlow dataset for 60 epochs and then fine-tuned for another 60 epochs. The learning rate initially is set to 0.001 and decayed by a factor of 2 after epoch 20, 32, 40, 48 and 56. Then, the trained model on SceneFlow is fine-tuned for 600 epochs on the mixed KITTI 2012 and KITTI 2015. For KITTI, the learning rate initially set to 0.001 and decayed to 0.0001 at 300th epoch. Furthermore, the generalization results on KITTI, ETH3D and Middlebury are obtained by the model trained only on SceneFlow.

4.3 Ablation Study

To evaluate the effectiveness of merging geometry information, an ablation experiment is conducted on SceneFlow dataset. To do so, we compare the performance of the baseline model with the full model. Here, the baseline is defined as the architecture without the coupling module and the output of the baseline is directly generated by the summation of the upper and lower branch. As shown in Table.1, the coupling module improves the performance of the baseline by reducing EPE from 0.72 to 0.60, which validates the efficiency of the proposed coupling module in improving the network performance.

4.4 Comparisons with State-of-the-art

SceneFlow. Table.2 demonstrates the performance of DCVSMNet on the SceneFlow test set compared to other state-of-the-art approaches. The methods are divided to two categories based on whether the networks are designed primarily for accuracy or for speed. The results show that DCVSMNet achieves remarkable accuracy (EPE = 0.60 px) on SceneFlow test set among the high speed methods and outperforms some complex stereo matching networks such as PSMNet [39], GwcNet [6], LEAStereo [7] and GANet [21].

KITTI 2012 and 2015. Table.3 demonstrates the official results on the KITTI 2012 and KITTI 2015 datasets. The results show that DCVSMNet outperforms other high speed methods in terms of accuracy by a large margin, at the cost of greater runtime. However, our model still performs better than JDCNet [18] which has an 80 ms inference time and some methods categorized as high accuracy networks such as SegStereo [22] and SSPCVNet [35]. —Further Figs.3 and 4 show the qualitative results for three scenes of KITTI 2012 and KITTI 2015 test set, which represents the capability of DCVSMNet in recovering thin and smooth structures.

4.5 Generalization Performance

Table.4 shows our model generalization results on KITTI 2012 [25], KITTI 2015 [26], Middlebury 2014[28] and ETH3D [27] compared to other non-real-time and real-time methods. Among high speed methods, our model achieves superior generalization performance. Furthermore, generalization results on ETH3D and Middlebury 2014 denote that our method not only generalizes better compared

Target	Method	EPE[px]	Time[ms]
Accuracy	CFNet [8]	0.97	180
	LEAStereo [7]	0.78	300
	GwcNet [6]	0.76	320
	GANet [21]	0.84	360
	PSMNet [39]	1.09	410
Speed	StereoNet [1]	1.10	15
	ADCPNet [38]	1.48	20
	BGNet [12]	1.17	25
	Coex [16]	0.68	27
	CGIStereo [20]	0.64	29
	EBStereo [41]	0.63	29
	MDCNet[17]	0.77	50
	DeepPrunerFast[15]	0.97	62
	AANet[9]	0.87	68
	JDCNet[18]	0.87	80
	DCVSMNet(ours)	0.60	67

Table 2: Evaluation on SceneFlow Dataset. The methods are categorized based on their design focus for accuracy or speed, we consider high speed methods to have an inference time $\leq 80ms$.

Target	Method	KITTI 2012						KITTI 2015			Time[ms]
		3-Noc	3-All	4-Noc	4-all	EPE noc	EPE all	D1-bg	D1-fg	D1-all	
Accuracy	CFNet [8]	1.23	1.58	0.92	1.18	0.4	0.5	1.54	3.56	1.88	180
	ACVNet [14]	1.13	1.47	0.86	1.12	0.4	0.5	1.37	3.07	1.65	200
	LEAStereo [7]	1.13	1.45	0.83	1.08	0.5	0.5	1.40	2.91	1.65	300
	EdgeStereo-V2 [23]	1.46	1.83	1.07	1.34	0.4	0.5	1.84	3.30	2.08	320
	CREStereo [15]	1.14	1.46	0.90	1.14	0.4	0.5	1.45	2.86	1.69	410
	SegStereo [22]	1.68	2.03	1.25	1.52	0.5	0.6	1.88	4.07	2.25	600
	SSPCVNet [35]	1.47	1.90	1.08	1.41	0.5	0.6	1.75	3.89	2.11	900
	CSPN [42]	1.19	1.53	0.93	1.19	-	-	1.51	2.88	1.74	1000
	GANet [21]	1.19	1.60	0.91	1.23	0.4	0.5	1.48	3.46	1.81	1800
	LaC+GANet [43]	1.05	1.42	0.80	1.09	0.4	0.5	1.44	2.83	1.67	1800
Speed	CGL-Stereo [20]	1.41	1.76	1.05	1.30	0.5	0.5	1.66	3.38	1.94	29*
	CoEx [16]	1.55	1.93	1.15	1.42	0.5	0.5	1.79	3.82	2.13	33*
	BGNet+ [12]	1.62	2.03	1.16	1.48	0.5	0.6	1.81	4.09	2.19	35*
	Fast-ACVNet+ [14]	1.45	1.85	1.06	1.36	0.5	0.5	1.70	3.53	2.01	45*
	DecNet [5]	-	-	-	-	-	-	2.07	3.87	2.37	50
	MDCNet[17]	1.54	1.97	-	-	-	-	1.76	-	2.08	50
	DeepPrunerFast [15]	-	-	-	-	-	-	2.32	3.91	2.59	50*
	HITNet[10]	1.41	1.89	1.14	1.53	0.4	0.5	1.74	3.20	1.98	54*
	DispNetC [29]	4.11	4.65	2.77	3.20	0.9	1.0	2.21	6.16	4.43	60
	AANet [9]	1.91	2.42	1.46	1.87	0.5	0.6	1.99	5.39	2.55	62
	JDCNet[18]	1.64	2.11	-	-	-	-	1.91	4.47	2.33	80
	DCVSMNet(ours)	1.30	1.67	0.96	1.23	0.5	0.5	1.60	3.33	1.89	67

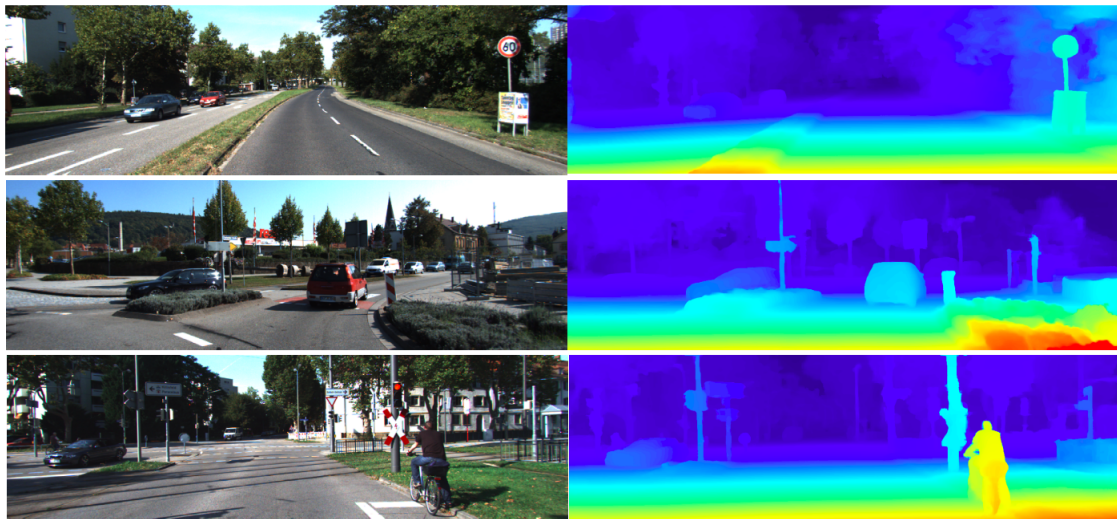
Table 3: Evaluation on KITTI Datasets. The methods are categorized based on their design focus for accuracy or speed (we consider high speed to mean an inference time ≤ 80 ms). * denotes the runtime is tested on our hardware (RTX 3090)



(a) Left image

(b) DCVSMNet

Figure 3: Qualitative results on KITTI 2012. Note how the model is able to recover fine details.



(a) Left image

(b) DCVSMNet

Figure 4: Qualitative results on KITTI 2015. Note how the model is able to recover fine details.

Target	Method	KITTI 2012 D1(%)	KITTI 2015 D1(%)	Middlebury bad 2.0(%)	ETH3D bad 1.0(%)
Accuracy	PSMNet[39]	6.0	6.3	15.8	9.8
	GANet[21]	10.1	11.7	20.3	14.1
	DSMNet[44]	6.2	6.5	13.8	6.2
	CFNet[8]	5.1	6.0	15.4	5.3
	STTR[45]	8.7	6.7	15.5	17.2
	FC-PSMNet[46]	5.3	5.8	15.1	9.3
	Graft-PSMNet[47]	4.3	4.8	9.7	7.7
Speed	DeepPrunerFast [15]	7.6	7.6	38.7	36.8
	BGNet[12]	12.5	11.7	24.7	22.6
	CoEx[16]	7.6	7.2	14.5	9.0
	CGI-Stereo[20]	6.0	5.8	13.5	6.3
	DCVSMNet(ours)	5.3	5.7	9.0	4.1

Table 4: Generalization performance on KITTI, Middlebury and ETH3D. All models are trained only on SceneFlow.

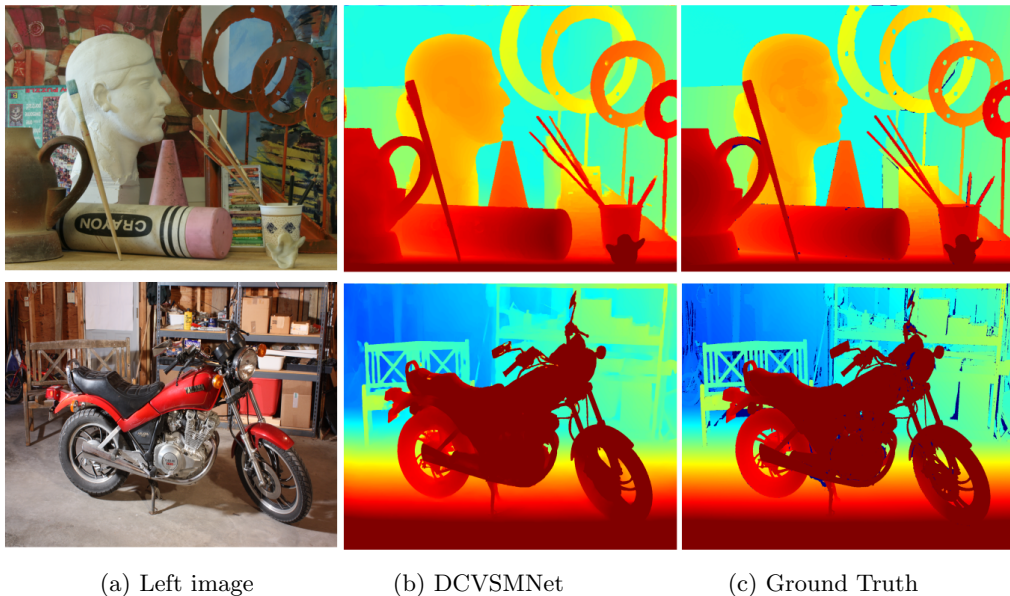


Figure 5: Generalization results of DCVSMNet on Middlebury 2014 dataset. Our model generalizes well to real-world scenarios when trained only on the synthetic SceneFlow dataset

to complex methods, but is also faster. Qualitative results are demonstrated in Figs.5 and 6 showing how well our method generalizes on real-world datasets.

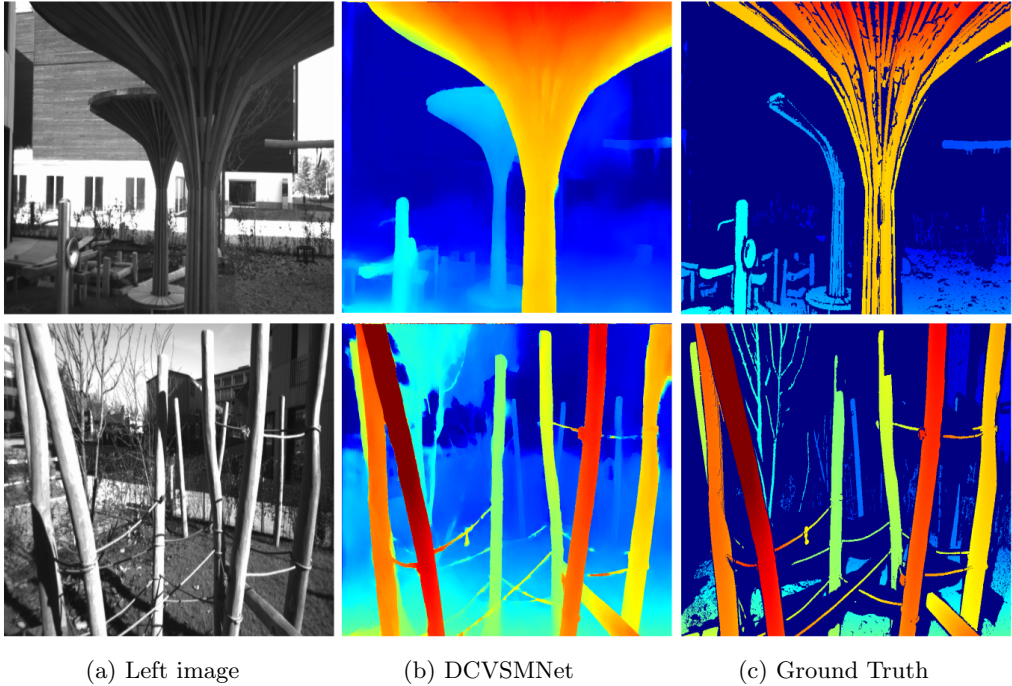


Figure 6: Generalization results of DCVSMNet on ETH3D dataset.

4.6 Computational Complexity Analysis

In the stereo matching pipeline, it is ideal to use cost volumes with few parameters while getting an acceptable accuracy for disparity estimation. In our approach, in contrast to GWCNet [6] which combines two large cost volumes and aggregates it using three hourglass networks, we construct two separate cost volumes with fewer parameters and aggregate them using two parallel hourglass networks which reduce the computation effort. Furthermore, we used the GWCNet [6] feature extraction backbone with 3.32 million parameters and build the cost volumes from last three layers of the feature extraction which have the same resolution. However, recent works such as ACVNet-Fast [14] and CGI-Stereo [20] adopted UNet-like feature extraction backbones with fewer parameters (such as MobileNet-v2[48] feature extraction backbone with 2.69 Million parameters) and reported promising results. Therefore, for the future work, we hope to increase the speed of our model by designing a light-weight UNet-like feature extraction and constructing the cost volumes at different resolutions to reduce the overall numbers of the network parameters and bring our network speed into the real-time zone.

5 Conclusion

The reported results show excellent performance on four datasets; KITTI 2012, KITTI 2015, Middlebury 2014, and ETH3D with competitive accuracy and strong generalization on real-world scenes. DCVSMNet is capable of recovering fine structures and outperforms state-of-the-art methods such as ACVNet-Fast [14] and CGI-Stereo [20] in terms of the accuracy. Further DCVSMNet exhibits remarkable generalization results compared to other methods categorized based on both their speed and accuracy. DCVSMNet owes its performance first to the two cost volumes built by two differ-

ent methods, which allow for storing richer and more variant matching information; and second to the coupling module that fuses the aggregated information from the upper and lower cost volumes enabling the network to learn more complex geometry and contextual information to balance the accuracy and speed. The DCVSMNet inference time of 67 ms is influenced by using two cost volumes and consequently the need for two 3D aggregation networks for processing, which limits the network use for applications with human-like performance requirement (40 ms) and raises challenges for implementation on edge devices with lower memory than high end GPUs. In future work, we plan to overcome this limitation by replacing the complex feature extractor with a lighter network to speed up the network, and prune the cost volumes by removing irrelevant information and preserving important matching parameters to reduce the chance of sacrificing accuracy caused by the lightweight feature extractor.

References

- [1] Sameh Khamis, Sean Fanello, Christoph Rhemann, Adarsh Kowdle, Julien Valentin, and Shahram Izadi. Stereonet: Guided hierarchical refinement for real-time edge-aware depth prediction. In *Proceedings of the European Conference on Computer Vision (ECCV)*, pages 573–590, 2018.
- [2] Kyoung Won Nam, Jeongyun Park, In Young Kim, and Kwang Gi Kim. Application of stereo-imaging technology to medical field. *Healthcare informatics research*, 18(3):158–163, 2012.
- [3] Yan Wang, Zihang Lai, Gao Huang, Brian H Wang, Laurens Van Der Maaten, Mark Campbell, and Kilian Q Weinberger. Anytime stereo image depth estimation on mobile devices. In *2019 international conference on robotics and automation (ICRA)*, pages 5893–5900. IEEE, 2019.
- [4] Cristhian A Aguilera, Cristhian Aguilera, Cristóbal A Navarro, and Angel D Sappa. Fast cnn stereo depth estimation through embedded gpu devices. *Sensors*, 20(11):3249, 2020.
- [5] Chengtang Yao, Yunde Jia, Huijun Di, Pengxiang Li, and Yuwei Wu. A decomposition model for stereo matching. In *Proceedings of the IEEE/CVF Conference on Computer Vision and Pattern Recognition*, pages 6091–6100, 2021.
- [6] Xiaoyang Guo, Kai Yang, Wukui Yang, Xiaogang Wang, and Hongsheng Li. Group-wise correlation stereo network. In *Proceedings of the IEEE/CVF conference on computer vision and pattern recognition*, pages 3273–3282, 2019.
- [7] Xuelian Cheng, Yiran Zhong, Mehrtash Harandi, Yuchao Dai, Xiaojun Chang, Hongdong Li, Tom Drummond, and Zongyuan Ge. Hierarchical neural architecture search for deep stereo matching. *Advances in Neural Information Processing Systems*, 33:22158–22169, 2020.
- [8] Zhelun Shen, Yuchao Dai, and Zhibo Rao. Cfnet: Cascade and fused cost volume for robust stereo matching. In *Proceedings of the IEEE/CVF Conference on Computer Vision and Pattern Recognition*, pages 13906–13915, 2021.
- [9] Haofei Xu and Juyong Zhang. Aanet: Adaptive aggregation network for efficient stereo matching. In *Proceedings of the IEEE/CVF Conference on Computer Vision and Pattern Recognition*, pages 1959–1968, 2020.
- [10] Vladimir Tankovich, Christian Hane, Yinda Zhang, Adarsh Kowdle, Sean Fanello, and Sofien Bouaziz. Hitnet: Hierarchical iterative tile refinement network for real-time stereo matching. In *Proceedings of the IEEE/CVF Conference on Computer Vision and Pattern Recognition*, pages 14362–14372, 2021.
- [11] Jiankun Li, Peisen Wang, Pengfei Xiong, Tao Cai, Ziwei Yan, Lei Yang, Jiangyu Liu, Haoqiang Fan, and Shuaicheng Liu. Practical stereo matching via cascaded recurrent network with adaptive correlation. In *Proceedings of the IEEE/CVF conference on computer vision and pattern recognition*, pages 16263–16272, 2022.
- [12] Bin Xu, Yuhua Xu, Xiaoli Yang, Wei Jia, and Yulan Guo. Bilateral grid learning for stereo matching networks. In *Proceedings of the IEEE/CVF Conference on Computer Vision and Pattern Recognition*, pages 12497–12506, 2021.
- [13] Wei Chen, Xiaogang Jia, Mingfei Wu, and Zhengfa Liang. Multi-dimensional cooperative network for stereo matching. *IEEE Robotics and Automation Letters*, 7(1):581–587, 2021.
- [14] Gangwei Xu, Yun Wang, Junda Cheng, Jinhui Tang, and Xin Yang. Accurate and efficient stereo matching via attention concatenation volume. *arXiv preprint arXiv:2209.12699*, 2022.

- [15] Shivam Duggal, Shenlong Wang, Wei-Chiu Ma, Rui Hu, and Raquel Urtasun. Deep-pruner: Learning efficient stereo matching via differentiable patchmatch. In *Proceedings of the IEEE/CVF international conference on computer vision*, pages 4384–4393, 2019.
- [16] Antyanta Bangunharcana, Jae Won Cho, Seokju Lee, In So Kweon, Kyung-Soo Kim, and Soohyun Kim. Correlate-and-excite: Real-time stereo matching via guided cost volume excitation. In *2021 IEEE/RSJ International Conference on Intelligent Robots and Systems (IROS)*, pages 3542–3548. IEEE, 2021.
- [17] Wei Chen, Xiaogang Jia, Mingfei Wu, and Zhengfa Liang. Multi-dimensional cooperative network for stereo matching. *IEEE Robotics and Automation Letters*, 7(1):581–587, 2021.
- [18] Xiaogang Jia, Wei Chen, Zhengfa Liang, Xin Luo, Mingfei Wu, Chen Li, Yulin He, Yusong Tan, and Libo Huang. A joint 2d-3d complementary network for stereo matching. *Sensors*, 21(4):1430, 2021.
- [19] Hengli Wang, Rui Fan, and Ming Liu. Scv-stereo: Learning stereo matching from a sparse cost volume. In *2021 IEEE International Conference on Image Processing (ICIP)*, pages 3203–3207. IEEE, 2021.
- [20] Gangwei Xu, Huan Zhou, and Xin Yang. Cgi-stereo: Accurate and real-time stereo matching via context and geometry interaction. *arXiv preprint arXiv:2301.02789*, 2023.
- [21] Feihu Zhang, Victor Prisacariu, Ruigang Yang, and Philip HS Torr. Ga-net: Guided aggregation net for end-to-end stereo matching. In *Proceedings of the IEEE/CVF Conference on Computer Vision and Pattern Recognition*, pages 185–194, 2019.
- [22] Guorun Yang, Hengshuang Zhao, Jianping Shi, Zhidong Deng, and Jiaya Jia. Segstereo: Exploiting semantic information for disparity estimation. In *Proceedings of the European conference on computer vision (ECCV)*, pages 636–651, 2018.
- [23] Xiao Song, Xu Zhao, Liangji Fang, Hanwen Hu, and Yizhou Yu. Edgestereo: An effective multi-task learning network for stereo matching and edge detection. *International Journal of Computer Vision*, 128:910–930, 2020.
- [24] Kyunghyun Cho, Bart Van Merriënboer, Caglar Gulcehre, Dzmitry Bahdanau, Fethi Bougares, Holger Schwenk, and Yoshua Bengio. Learning phrase representations using rnn encoder-decoder for statistical machine translation. *arXiv preprint arXiv:1406.1078*, 2014.
- [25] Andreas Geiger, Philip Lenz, and Raquel Urtasun. Are we ready for autonomous driving? the kitti vision benchmark suite. In *2012 IEEE conference on computer vision and pattern recognition*, pages 3354–3361. IEEE, 2012.
- [26] Moritz Menze and Andreas Geiger. Object scene flow for autonomous vehicles. In *Proceedings of the IEEE conference on computer vision and pattern recognition*, pages 3061–3070, 2015.
- [27] Thomas Schops, Johannes L Schonberger, Silvano Galliani, Torsten Sattler, Konrad Schindler, Marc Pollefeys, and Andreas Geiger. A multi-view stereo benchmark with high-resolution images and multi-camera videos. In *Proceedings of the IEEE conference on computer vision and pattern recognition*, pages 3260–3269, 2017.
- [28] Daniel Scharstein, Heiko Hirschmüller, York Kitajima, Greg Krathwohl, Nera Nešić, Xi Wang, and Porter Westling. High-resolution stereo datasets with subpixel-accurate ground truth. In *Pattern Recognition: 36th German Conference, GCPR 2014, Münster, Germany, September 2-5, 2014, Proceedings 36*, pages 31–42. Springer, 2014.

- [29] Nikolaus Mayer, Eddy Ilg, Philip Hausser, Philipp Fischer, Daniel Cremers, Alexey Dosovitskiy, and Thomas Brox. A large dataset to train convolutional networks for disparity, optical flow, and scene flow estimation. In *Proceedings of the IEEE conference on computer vision and pattern recognition*, pages 4040–4048, 2016.
- [30] Liang-Chieh Chen, George Papandreou, Iasonas Kokkinos, Kevin Murphy, and Alan L Yuille. Deeplab: Semantic image segmentation with deep convolutional nets, atrous convolution, and fully connected crfs. *IEEE transactions on pattern analysis and machine intelligence*, 40(4): 834–848, 2017.
- [31] Anurag Ranjan and Michael J Black. Optical flow estimation using a spatial pyramid network. In *Proceedings of the IEEE conference on computer vision and pattern recognition*, pages 4161–4170, 2017.
- [32] Deqing Sun, Xiaodong Yang, Ming-Yu Liu, and Jan Kautz. Pwc-net: Cnns for optical flow using pyramid, warping, and cost volume. In *Proceedings of the IEEE conference on computer vision and pattern recognition*, pages 8934–8943, 2018.
- [33] Jia-Ren Chang, Pei-Chun Chang, and Yong-Sheng Chen. Attention-aware feature aggregation for real-time stereo matching on edge devices. In *Proceedings of the Asian Conference on Computer Vision*, 2020.
- [34] Pier Luigi Dovesi, Matteo Poggi, Lorenzo Andraghetti, Miquel Martí, Hedvig Kjellström, Alessandro Pieropan, and Stefano Mattoccia. Real-time semantic stereo matching. In *2020 IEEE international conference on robotics and automation (ICRA)*, pages 10780–10787. IEEE, 2020.
- [35] Zhenyao Wu, Xinyi Wu, Xiaoping Zhang, Song Wang, and Lili Ju. Semantic stereo matching with pyramid cost volumes. In *Proceedings of the IEEE/CVF international conference on computer vision*, pages 7484–7493, 2019.
- [36] Jie Wang, Sunjie Zhang, Yongxiong Wang, and Zhengyu Zhu. Learning efficient multi-task stereo matching network with richer feature information. *Neurocomputing*, 421:151–160, 2021. ISSN 0925-2312. doi: <https://doi.org/10.1016/j.neucom.2020.08.010>. URL <https://www.sciencedirect.com/science/article/pii/S0925231220312704>.
- [37] Aixin Chong, Hui Yin, Yanting Liu, Jin Wan, Zhihao Liu, and Ming Han. Multi-hierarchy feature extraction and multi-step cost aggregation for stereo matching. *Neurocomputing*, 492: 601–611, 2022. ISSN 0925-2312. doi: <https://doi.org/10.1016/j.neucom.2021.12.052>. URL <https://www.sciencedirect.com/science/article/pii/S0925231221018890>.
- [38] He Dai, Xuchong Zhang, Yongli Zhao, and Hongbin Sun. Adcpnet: Adaptive disparity candidates prediction network for efficient real-time stereo matching. *arXiv preprint arXiv:2011.09023*, 2020.
- [39] Jia-Ren Chang and Yong-Sheng Chen. Pyramid stereo matching network. In *Proceedings of the IEEE conference on computer vision and pattern recognition*, pages 5410–5418, 2018.
- [40] Diederik P Kingma and Jimmy Ba. Adam: A method for stochastic optimization. *arXiv preprint arXiv:1412.6980*, 2014.
- [41] Weijie Bi, Ming Chen, Dongliu Wu, and Shenglian Lu. Ebstereo: edge-based loss function for real-time stereo matching. *The Visual Computer*, pages 1–12, 2023.

- [42] Xinjing Cheng, Peng Wang, and Ruigang Yang. Learning depth with convolutional spatial propagation network. *IEEE transactions on pattern analysis and machine intelligence*, 42(10): 2361–2379, 2019.
- [43] Biyang Liu, Huimin Yu, and Yangqi Long. Local similarity pattern and cost self-reassembling for deep stereo matching networks. In *Proceedings of the AAAI Conference on Artificial Intelligence*, volume 36, pages 1647–1655, 2022.
- [44] Feihu Zhang, Xiaojuan Qi, Ruigang Yang, Victor Prisacariu, Benjamin Wah, and Philip Torr. Domain-invariant stereo matching networks. In *Computer Vision–ECCV 2020: 16th European Conference, Glasgow, UK, August 23–28, 2020, Proceedings, Part II 16*, pages 420–439. Springer, 2020.
- [45] Zhaoshuo Li, Xingtong Liu, Nathan Drenkow, Andy Ding, Francis X Creighton, Russell H Taylor, and Mathias Unberath. Revisiting stereo depth estimation from a sequence-to-sequence perspective with transformers. In *Proceedings of the IEEE/CVF international conference on computer vision*, pages 6197–6206, 2021.
- [46] Jiawei Zhang, Xiang Wang, Xiao Bai, Chen Wang, Lei Huang, Yimin Chen, Lin Gu, Jun Zhou, Tatsuya Harada, and Edwin R Hancock. Revisiting domain generalized stereo matching networks from a feature consistency perspective. In *Proceedings of the IEEE/CVF Conference on Computer Vision and Pattern Recognition*, pages 13001–13011, 2022.
- [47] Biyang Liu, Huimin Yu, and Guodong Qi. Graftnet: Towards domain generalized stereo matching with a broad-spectrum and task-oriented feature. In *Proceedings of the IEEE/CVF Conference on Computer Vision and Pattern Recognition*, pages 13012–13021, 2022.
- [48] Mark Sandler, Andrew Howard, Menglong Zhu, Andrey Zhmoginov, and Liang-Chieh Chen. Mobilenetv2: Inverted residuals and linear bottlenecks. In *Proceedings of the IEEE conference on computer vision and pattern recognition*, pages 4510–4520, 2018.